DOI: 10.1002/ppap.201500200

Article type: Full Paper

Sulfur-rich Organic Films deposited by Plasma- and Vacuum-ultraviolet (VUV) Photo-polymerization

Evelyne Kasparek, Jason R. Tavares, Michael R. Wertheimer, Pierre-Luc Girard-Lauriault*

ĐĐĐĐĐĐĐĐĐ

E. Kasparek, P.-L. Girard-Lauriault
Plasma Processing Laboratory, Department of Chemical Engineering,
McGill University, Montreal, QC H3A 2B2, Canada
Email: pierre-luc.girard-lauriault@mcgill.ca
J. R. Tavares
Photochemical Surface Engineering Laboratory, Department of Chemical Engineering, ƒcole Polytechnique de MontrŽal, MontrŽal, QC H3C 3A7, Canada
M. R. Wertheimer
Groupe des couches minces (GCM) and Department of Engineering Physics, ƒcole Polytechnique de MontrŽal, MontrŽal, QC H3C 3A7, Canada

ĐĐĐĐĐĐĐĐĐ

Abstract

Thiol (SH)-terminated surfaces have been progressively gaining interest over the past years as a consequence of their widespread potential applications. Here, SH-terminated thin films have been prepared by 'co-polymerizing' gas mixtures comprising ethylene (C_2H_4) or butadiene (C_4H_6) with hydrogen sulfide (H_2S). This has been accomplished by either vacuum-ultraviolet (VUV) irradiation of the flowing gas mixtures with near-monochromatic radiation from a Kr lamp, or by low-pressure r.f. plasma-enhanced chemical vapor deposition (PECVD). Varying the gas mixture ratio, *R*, allows one to control the films' sulfur content as well as the thiol concentration [-SH]. The deposits were characterized by X-ray photoelectron spectroscopy (XPS), before and after chemical derivatization with *N*-ethylmaleimide, and by IRRAS-FTIR. VUV- and plasma-prepared coatings were found to possess very similar structures and characteristics, showing chemically bonded sulfur concentrations, [S], up to 48 at. % and [-SH] up to 3%. All coatings remained essentially unchanged in thickness after immersion in water for 24 h.

Introduction

General introduction

Thiol (SH)-terminated surfaces have been gaining interest over the past years, to promote adhesion of gold layers[1] and nanoparticles,[2] and for immobilization of biomolecules like DNA,[3] carbohydrates,[4] and proteins.[5] In particular, protein immobilization can be accomplished by covalently attaching them to the surface through thiol-ene click chemistry. Such covalent attachment is important because it ensures homogeneous surface coverage and accessibility to the active site(s) of the protein;[5-6] it therefore appears superior to electrostatic attachment, the presumed surface interaction for amine (NH_2)-rich organic thin films.[7]

So far, SH-terminated surfaces have been synthesized using wet-chemical approaches comprising several different steps,[5-6] with different solvents and long reaction times. An alternative solvent-free, single-step process is low-pressure (LP) plasma deposition of thin coatings, something that has been accomplished using single volatile organic precursors with the desired functionality.[3a, 8] Additionally, binary gas mixtures of SO_2 and hydrogen have recently shown to be able to create thiol containing surfaces,[9] but no complete characterization of these surfaces was performed. In this study, *binary* gas mixtures comprising a hydrocarbon, here ethylene (C_2H_4) or 1,3-butadiene (C_4H_6), and hydrogen sulfide (H_2S) are used to create SH-terminated surfaces. This approach of using feed-gas with controllable gas mixture ratios, *R*, has been demonstrated to be at least equal, if not superior,[7b-d, 10] to the single-molecule precursor for nitrogen-containing coatings (amongst others),[17-19,23-25] as *R* allows for increased versatility to achieve coatings with tailored properties. Although binary-mixture feeds ~~were pioneered by Hegemann and~~

~~coworkers~~ have already been used by Yasuda et al.[11] and more recently by Hegemann and coworkers,[12] neither they, nor any other group, have so far reported using H_2S as co-reagent, to the best of our knowledge.

For a number of years, nitrogen (N)- [or better, amine (NH_2)]-rich polymer surfaces have been created using low-pressure plasma polymerization of C_2H_4-ammonia (NH_3) mixtures.[7b, 7d, 10b] More recently, vacuum-ultraviolet (VUV, $\lambda \leq 200$ nm)-assisted photo-polymerization of such mixtures using quasi-monochromatic sources[7d, 10a] has also been demonstrated. In essence, VUV-assisted processing retains only one energy-source component of the plasma, the VUV photons, to carry out (photo-) chemistry, thus potentially allowing for better control of the overall process. Indeed, VUV-based deposits tend to possess higher amine concentrations, [-NH_2], likely due to more specific and selective reactions occurring via mono-energetic photons; ò hotó electrons, the main originators of chemical reactions in low-pressure plasmas, necessarily possess a broad, Maxwell-Boltzmann-like energy distribution.[7c, 7d, 13] In addition, VUV radiation can more readily promote intermolecular cross-linking, leading to more stable films compared with their low-pressure plasma counterparts.[7c]

The purpose of the present research is to compare S-containing organic thin films created by photo- and plasma-assisted polymerization of C_2H_4 or C_4H_6 with H_2S, and to gain insight into the reaction pathways that favor high thiol concentrations and coating stability. It is useful, however, to first present some introduction into the photochemistry of small molecules,[14] particularly those relating to the above-listed gaseous reagents.

VUV photolysis of C_2H_4, C_4H_6 and H_2S

In order to achieve appreciable sulfur (S) incorporation into the organic thin films, absorption of photons in the precursor gas mixtures (and thus, their photo-dissociation) must be significant. Absorption coefficients, *k*, should ideally be high at the VUV emission wavelength of the KrL lamp used here (see Experimental section), λ_{Kr} = 123.6 nm. **Figure 1** shows plots of *k* for the three precursor gases as a function of the wavelength, λ, as well as λ_{Kr}, where all three *k* values are seen to be very high, favoring bond scissions and formation of reactive radicals for film-forming reactions.

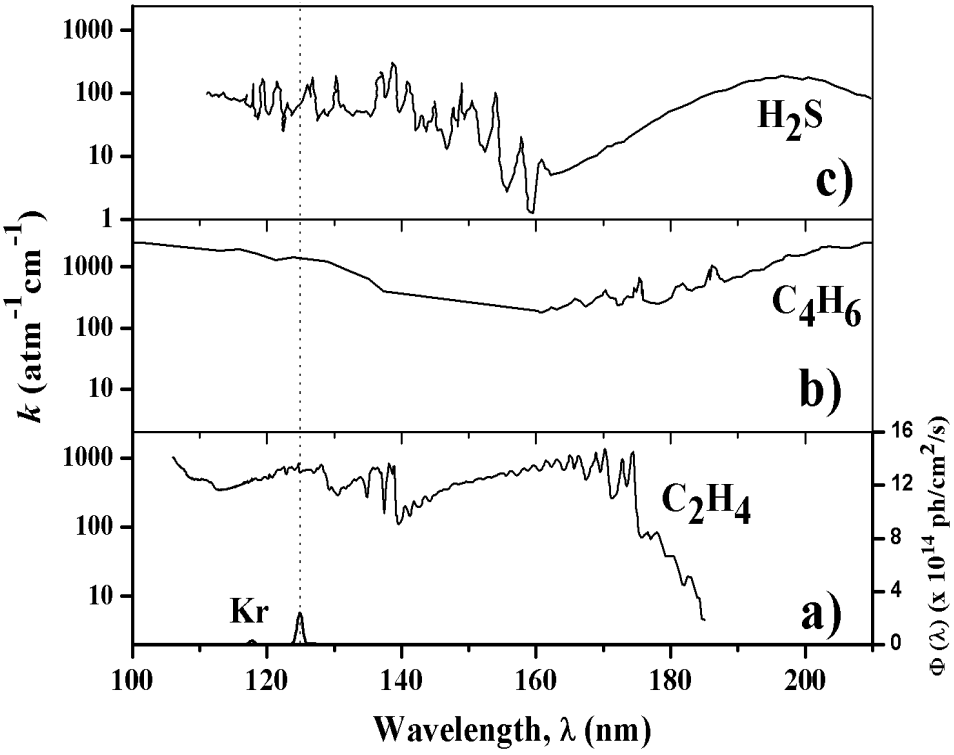

Figure 1 *VUV absorption coefficients, k (atm^{-1}cm^{-1}, base e), of gaseous a) C_2H_4,* [15] *b) C_4H_6* [16] *and c) H_2S;*[14] *the wavelength of the Kr (λ_{Kr}= 123.6 nm) resonant VUV lamps is also shown.*

Two primary dissociative processes of similar importance have been reported for ethylene, C_2H_4, both leading to the formation of acetylene:[7c, 7d, 10b, 13],[15a]

$$!_{"}\#_{\$}\,\%\,\&'\,(\;!_{"}\#_{"}\,\%\,\#_{"} \qquad \textbf{(1)}$$

$$!_{"}\#_{\$}\,\%\,\&'\,(\;)!_{"}\#_{*}^{+}\,\%\,\#,\,(\;!_{"}\#_{"}\,\%\,\#_{"} \qquad \textbf{(2)}$$

Secondary reactions include those of H to form ethyl radicals, $C_2H_5\cdot$, and reaction of the latter to form higher species, such as C_4H_{10}, C_2H_4 and C_2H_6.

Photolytic reactions of butadiene, C_4H_6, include the formation of hydrogen, radicals and other unsaturated molecules. Additionally, low structural isomers of 1,3-butadiene can be formed, namely 1,2-butadiene, cyclobutadiene and bicyclobutadiene. Five primary reaction channels have been reported for the dissociation of 1,3-butadiene, including three radical (**(3)-(5)**) and two molecular (**(6)-(7)**) channels:[17]

$$!_{\$}\#_{-}\,\%\,\&'\,(\;!_{*}\#_{*}\,.\,\%\,.\,!\,\#_{*} \qquad \textbf{(3)}$$

$$!_{\$}\#_{-}\,\%\,\&'\,(\;!_{\$}\#_{/}\,.\,\%\,.\,\# \qquad \textbf{(4)}$$

$$!_{\$}\#_{-}\,\%\,\&'\,(\;!_{"}\#_{*}\,.\,\%!_{"}\#_{*}\,. \qquad \textbf{(5)}$$

$$!_{\$}\#_{-}\,\%\,\&'\,(\;!_{"}\#_{\$}\,\%\,!_{"}\#_{"} \qquad \textbf{(6)}$$

$$!_{\$}\#_{-}\,\%\,\&'\,(\;!_{\$}\#_{\$}\,\%\,\#_{"} \qquad \textbf{(7)}$$

The primary photo-reaction of H_2S at short wavelengths (λ < 317 nm) is predominantly the production of hydrogen atoms and SH· radicals:[14]

$$\#_2 0 \rightarrow \& ' (\ + \ \#.\%\#0. \quad \textbf{(8)}$$

Secondary reactions include:

$$\#.\%\#_2 0 (\#_2 \% \#0. \quad \textbf{(9)}$$

$$1\#0.(\ \#_2 0 \% 0 \quad \textbf{(10)}$$

$$1\#0.(\ \#0_2 .\%\#. \quad \textbf{(11)}$$

$$1\#0.(\ 0_2 \% \#_2 \quad \textbf{(12)}$$

$$1\#0.(\ \#_2 0_2 \quad \textbf{(13)}$$

Recombination of radicals from the photolysis of C_2H_4-H_2S or C_4H_6-H_2S mixtures then clearly leads to reaction pathways that form the polymer-like thin films.

Experimental Section

VUV photo-polymerization

The experimental set-ups shown in **Figure 2** are housed in a glovebox (see photograph in **Figure 2a**), on account of the highly toxic nature of H_2S; the reactor

used for VUV photo-chemical experiments, shown in **Figure 2c**, is very similar to that of Truica-Marasescu et al.[7d, 10a, 18]

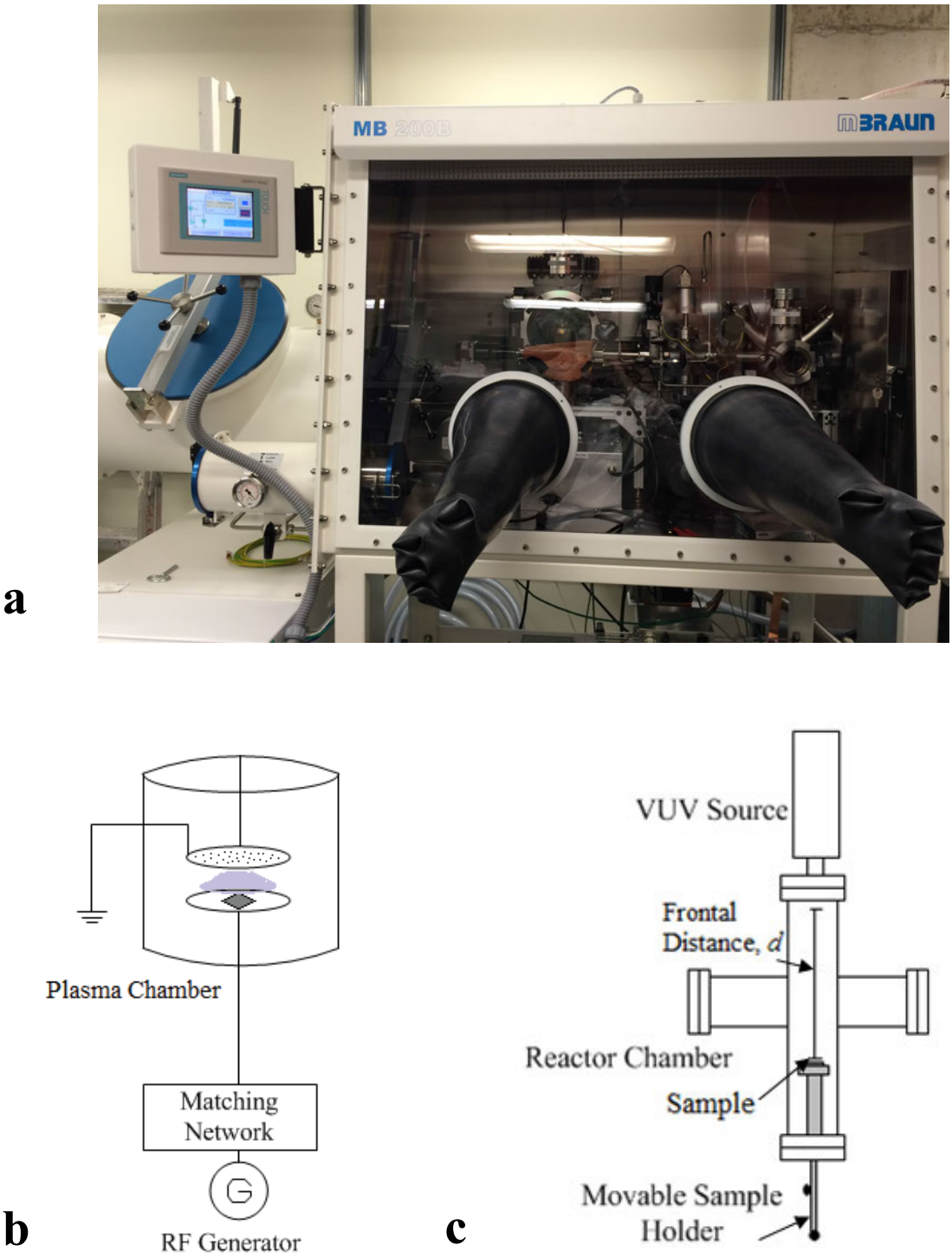

Figure 2 *(a) Photograph showing the experimental setups inside a glovebox (top) and schematic views (bottom) of (b) the low-pressure r.f. reactor; and (c) the vacuum*

ultra-violet (VUV) photo-chemical reactor, used for depositing sulfur-rich thin organic thin films, L-PPE:S, L-PPB:S and UV-PE:S, UV-PB:S, respectively.

Briefly, it consists of a stainless steel ÔÔcrossÒÕ chamber, evacuated to high vacuum using a turbo-molecular pump supported by a two-stage rotary vane pump (base pressure $p = 10^{-5}$ Pa). As in previous experiments,[7b-d, 10b, 10c, 13] the operating pressure during deposition was maintained near p = 13 Pa (100 mTorr). The flow rate of the high-purity hydrocarbon source gases C_2H_4 (99.999%, Megs Inc., Montreal, QC, Canada), F_{C2H4}, or C_4H_6 (99.8%, Megs Inc., Montreal), F_{C4H6}, was kept constant at 10 sccm using mass flow controllers (Brooks Instruments, Hatfield, PA), while the flow rate of H_2S (99.5%, Megs Inc., Montreal), F_{H2S}, was varied between 0 and 15 sccm, also using a mass flow controller; this yielded values of R (e.g. F_{H2S}/F_{C4H6}) ranging from 0 to 1.5. The polymer-like[19] coatings resulting from the photo-chemical reactions, henceforth designated ÔÔUV-PE:SÒÕ (for ÔÔultraviolet- polymerized sulfurized ethyleneÒÕ) and ÒUV-PB:SÓ (for Òultraviolet- polymerized sulfurized butadieneÓ), were deposited on 500 μm-thick (100) p-type silicon wafers (University Wafer, Boston, MA, USA), or on glass slides with a thin (ca. 100 nm) Au coating, substrates being placed at a frontal distance, d, of 10 mm facing the VUV source. The exact value of d is important, because radiation intensity decreases as d^{-2}. [18a] We used a non-coherent commercial VUV (ÒKrLÓ) lamp (Resonance Ltd., Barrie, ON, Canada), based on an electrodeless radio-frequency (r.f., 100 MHz)-powered discharge plasma in krypton (Kr) gas at low pressure: the Kr is contained in a Pyrex ampoule sealed with a MgF_2 window (cut-off wavelength, λ = 112 nm), as described in further detail elsewhere[7d, 10a, 18a]; as already mentioned in the section on VUV

photolysis, its (resonant) emission wavelength is λ_{Kr} = 123.6 nm (photon energy ca. 10 eV).

Finally, it is appropriate to mention that plasma and VUV effective power values at the substrate during deposition are of comparable magnitude, ca. 0.1 W/cm^{-2}.

Plasma polymerization

For comparison, we have also used low-pressure r.f. plasma to deposit thin plasma polymer (PP) films with the same gas mixtures and the same *R* values, henceforth-designated ÔÔlow-pressure plasma-polymerized, sulfurized ethyleneÕÕ, L-PPE:S, or Òlow-pressure plasma-polymerized, sulfurized butadieneÓ, L-PPB:S. Depositions were performed in a cylindrical stainless steel vacuum chamber (20 cm in diameter and 50 cm in height), with a disc-shaped powered electrode (10 cm in diameter) onto which substrates were placed (**Figure 2b**). A showerhead gas distributor and the metallic chamber walls served as the grounded electrode. L-PPE:S and L-PPB:S films were deposited under mild plasma conditions (r.f. power, *P* =20 W, resulting in a bias voltage of ca. -40 V, gas pressure, *p* = 80 Pa = 600 mTorr).

Characterization studies

All deposits were characterized by X-ray photoelectron spectroscopy (XPS), performed in a Thermo Scientific K-Alpha^{TM} instrument (Waltham, MA, USA), using a monochromatic Al Kα radiation source (*hν* = 1486.6 eV). The elemental composition (in atomic %, at. %) and the chemical environment of the elements in the deposits were obtained by XPS analyses (survey- and high-resolution, HR, spectra). Survey spectra were acquired at a pass energy of 160 eV, a dwell time of 200 ms and energy steps of 1 eV. HR spectra were acquired at a pass energy of 20 eV, a dwell

time of 200 ms and energy steps of 0.1 eV. No evidence of X-ray induced damage was ever observed, based on observation of the C1s spectra before and after analyses. Spectra were acquired at 0° emission angles, normal to the sample surface; possible charging was corrected by referencing all peaks to the C1s peak at binding energy (BE) = 285.0 eV. The constituent elements were quantified from broad-scan spectra using 2.3.16 PR 1.6 Casa XPS software, by integrating the areas under relevant peaks after a Shirley-type background subtraction, and by using sensitivity factors from the Wagner table. C1s spectra were peak-fitted according to BEs of the different possible chemical bonds, before and after derivatization reactions (**Table 1**).

Table 1: *Assignment of expected chemical bonds to binding energies (BE) of peaks labelled C1-C4 for sulfur-rich thin films (a) as-deposited, and after (b) derivatization with N-ethylmaleimide.*

C1s peak assignments				
Peak label	**a) As-deposited**		**b) After derivatization**	
	Possible Chemical Bond	Peak BE (eV)	Possible Chemical Bond	Peak BE (eV)
C1	C-C, C-H	~~284.8±0.2~~ 285[20]	C-C, C-H	~~284.8±0.2~~ 285[20]
C2	C-S	285.3±0.2[20]	C-S	285.3±0.2[20]
C3			C-OR	286.5±0.2[20]
C4			N-C=O	288.1±0.2[20]

Fourier-transform (reflection-absorption) infrared (FTIR) spectroscopy (Digilab FTS7000-UMA600 instrument, equipped with a microscope and MCT detector) was used for further chemical characterization. Spectra were obtained in transmittance mode, with the gold coating acting as the reflector; all spectra were acquired at a resolution of 1 cm^{-1}. A blank, gold-coated microscope slide was used to acquire background spectra.

Chemical derivatization with *N*-ethylmaleimide

To quantify thiol concentrations, [SH], we used the chemical derivatization reaction with *N*-ethylmaleimide (98%, BioShop Canada, Inc., Burlington, ON, Canada), as recently described by Thiry et al..[8a] The reaction mechanism is shown in **Scheme 1**, wherein *N*-ethylmaleimide reacts selectively with SH-groups via a nucleophilic addition between the S atom and the double bond in the maleimide structure (thiol-ene click reaction), forming a stable thio-ether.

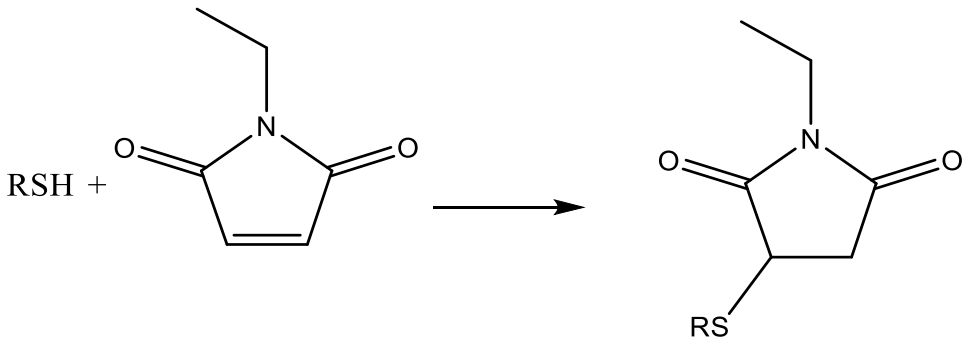

Scheme 1 *Derivatization reaction between a thiol and N-ethylmaleimide.*

In a typical experiment, the derivatization reaction was carried out in a phosphate buffer solution at pH = 7, where the *N*-ethylmaleimide concentration was fixed at 0.1 M. The samples were immersed in this solution for 40 h, following which they were

rinsed in simple buffer solution for 5 min to eliminate any unreacted molecules, then dried under a flow of dry nitrogen.

XPS survey spectra were obtained before and after performing the derivatization reaction, allowing nitrogen, [N], and carbon, [C], concentrations to be quantified; the concentration of thiol groups, [SH], is then calculated as follows:

$$[0\#]\ 2\ \frac{[3]}{[!]\ 4\ 5[3]}\ 6788\%(:) \qquad \textbf{(14)}$$

Deposition rates

The deposition rates, *r* (in nm/min), were determined from thickness, *T*, measurements as a function of the duration of deposition by evaluating the depth of a ò scratch ó produced by a sharp needle using a surface profilometer (Veeco Dektak^{3}ST-Surface Profile Measuring System, Plainview, NY, USA).

Stability studies

The stability against dissolution of all coatings was examined after immersion in Milli-Q water or toluene for 24 h. Profilometry ~~(Veeco Dektak^{3}ST-Surface Profile Measuring System, Plainview, NY, USA)~~ was used to measure possible changes in film thickness, *T*, (before and after immersion on three different points, ΔT, in %) due to partial dissolution. The rationale for using these two solvents will be presented later in this text.

Results and Discussion

Deposition kinetics

Figure 3 shows plots of deposition rates, *r* (in nm/min) of the all coatings, as a function of the gas mixture ratio, *R*.

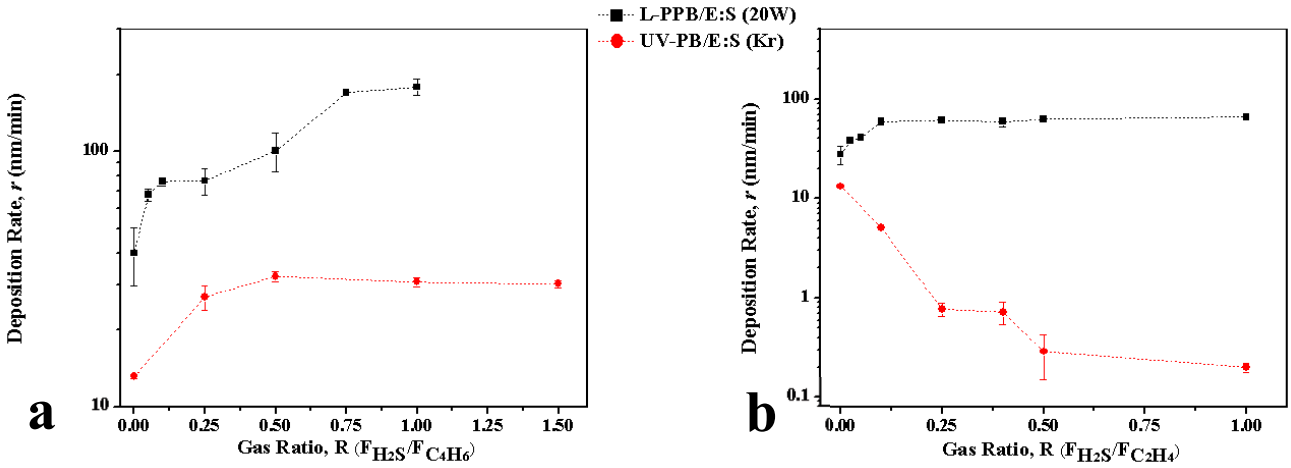

Figure 3 *Deposition rates, r, of: a) L-PPB:S (squares, 20 W) and UV-PB:S (circles, KrL) and b) L-PPE:S (squares, 20 W) and, UV-PE:S (circles, KrL) as a function of gas mixture ratio, R. Error bars show standard deviation of three measurements. The lines are to guide the reader s eye.*

The most striking features noted are:

(i) When comparing photo- and plasma-polymerized films for both source gases, it can be observed that v~~V~~alues of *r* for the VUV-deposited films are significantly lower than those from plasma polymerization. This ~~may be~~ is due to higher efficiency of radical creation by plasma compared with VUV irradiation, as first pointed out by Truica et al.;[7d]

(ii) Comparing the two different source gases, it can be noted that b~~B~~utadiene-based *r* values are much higher than those with ethylene, likely due to *two* double bonds and twice as many C atoms in the former molecule. These features render the butadiene molecule more reactive than ethylene, which is also understandable when looking at equations (**3**)-(**8**). A related finding

occurred when acetylene, C_2H_2, was used as source gas.[10c] In addition, when using C_4H_6, no drop in *r* was observed, even at higher *R* values; this is somewhat surprising, because *r* decreased substantially in previous experiments with C_2H_4 and N- or O-containing gas mixtures.[7c, 7d, 10b, 13] In those previous works it has been shown that NH_3, for example, acts as an etchant for organic materials, because with increasing *R* values atomic H is released during fragmentation, leading to a decrease in *r*. [10c] Of course, the relative concentration of C_xH_y radicals decreases with rising *R* when *p* and F_{CxHy} ~~is~~ are kept constant. ~~Furthermore, the increasing release of H atoms during fragmentation has a strong etching effect~~. Therefore, the decrease in *r* with increasing *R* when using C_2H_4, as observed in previous experiments, comes as no surprise.[7d, 10a] The near-constant *r* values when using H_2S (except for UV-PE:S films) ~~for C_4H_6~~ show~~s~~ that deposition (not etching) dominates, even at higher *R*.

Compositions of deposited films

Figure 4 shows surface-near sulfur concentrations, [S], from broad-scan XPS, as a function of *R*, for the four different types of coatings.

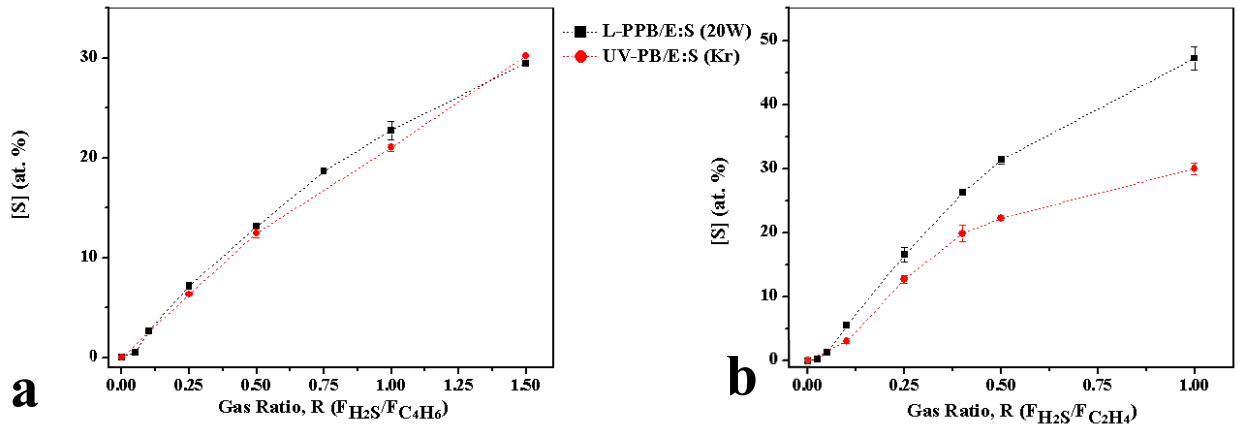

Figure 4 *Surface-near sulfur concentrations, [S] (in at.- %), as measured by XPS of a) L-PPB:S (squares, 20 W) and UV-PB:S (circles, KrL) and b) L-PPE:S (squares, 20 W) and UV-PE:S (circles, KrL) as a function of gas mixture ratio, R. The lines are to guide the reader s eye.*

[S] is seen to increase monotonically with rising *R*; for the case of C_4H_6 (**Figure 4a**), no apparent distinction can be made between the photo- and plasma-polymerized films, and [S] values up to 30 at. % could be obtained. The similarity between photo- and plasma-polymerized films ~~This~~ had previously been observed for N-containing films based on C_2H_4.[7d] In contrast, here, when using the latter hydrocarbon, PP films yield higher [S] values, up to 48 at. % (**Figure 4b**). Similar results were also reported for O-containing films,[13] a clear indication that the plasma- and VUV-based chemistries are quite different and complex. Further, surface oxygen concentrations were always below 5 at. % (results not shown), which could be an indication that these films are more stable towards ageing compared to nitrogen containing films.

Figure 5, [SH] values obtained from derivatization experiments, as a function of *R* for the four different types of films, is seen to differ from [S] data, **Figure 4**. While **Figure 4** shows relatively minor differences among [S] between the photo- and plasma-polymerized films, this is not the case for [SH].

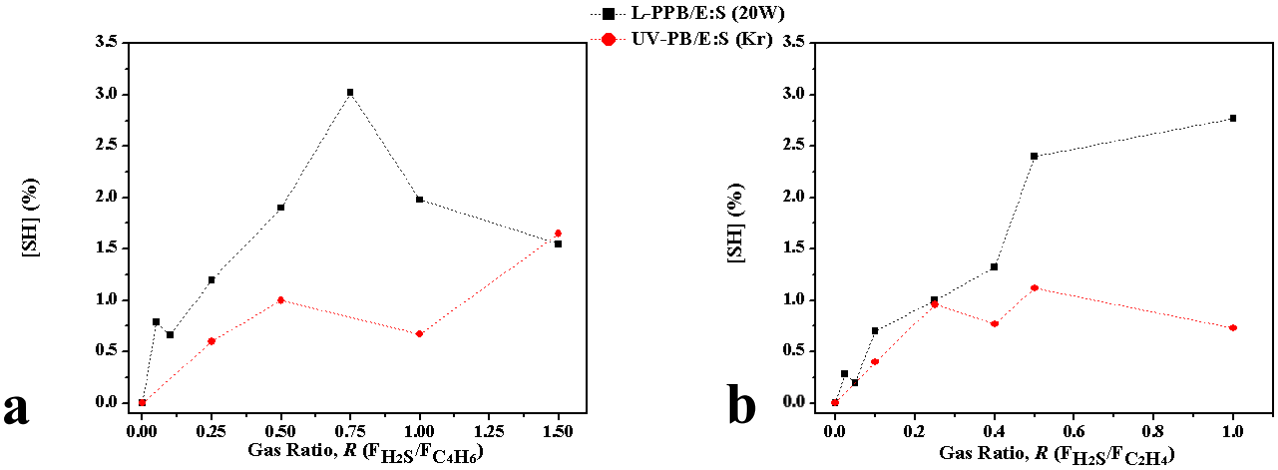

Figure 5 *Thiol concentrations, [SH] (in %), determined using chemical derivatization XPS: a) L-PPB:S (squares, 20 W) and UV-PB:S (circles, KrL) and b) L-PPE:S (squares, 20 W) and UV-PE:S (circles, KrL) as a function of gas mixture ratio, R. The lines are to guide the reader s eye.*

Contrary to expectations and to results for N-containing films,[7c, 7d] L-PPB/E:S coatings are seen to be richer in thiols (up to 3%) than their UV-PB/E:S counterparts (only 1.6%). This is surprising since the retention of functional groups is believed to be limited in plasma polymerization due to heterogeneous reactions of gas phase species competing at the growing surface. The reason of this opposed result is under current investigation. For comparison, Thiry et al.[8a] reported [SH] values up to 5 %, using the SH-containing precursor molecule, propanethiol.

Infrared spectra

Figure 6 shows selected FTIR reflection-absorption (IRRAS) spectra of L-PPB:S (**Figure 6a**) and UV-PB:S (**Figure 6b**) films at two different *R* values, *R* = 0 and *R* = 1.

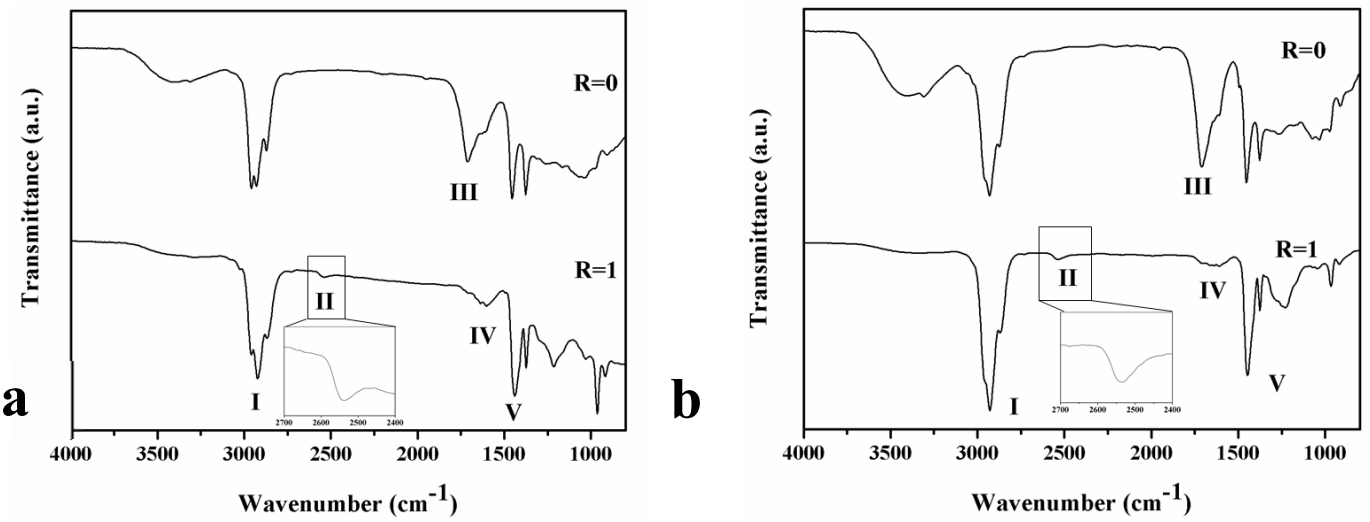

Figure 6 *FTIR reflection/absorption spectra (IRRAS) of a) L-PPB:S and b) UV-PB :S films. Comparison between L:PPB:S (20W) and UV-PB:S (KrL) IRRAS deposited with R values (R= 0 and R=1, [S]~22 at. %). See Table 2 for assignments of bands I , II , III , IV and V .*

Peak assignments in the principal absorption regions, labeled ÒI - VÓ, are listed in **Table 2**.

Table 2: *Infrared peak assignments of sulfur-containing thin films.*[21]

Bands	Peak (cm^{-1})	Peak assignment
I	2969-2965	Antisymmetric CH_3 stretch
	2929-2912	Antisymmetric CH_2 stretch
	2884-2883	Symmetric CH_3 stretch
	2861-2849	Symmetric CH_2 stretch
II	2590-2560	SH stretch
III	1725-1700	C=O stretch

IV	1648-1638	C=C stretch
V	1473-1443	CH_3, CH_2 deformations
	1466-1465	CH_3 deformation
	1385-1368	CH_3 symmetric deformation

Unfortunately, C-S and C-S-H stretching vibrations tend to give rise to very weak absorptions in the infrared spectrum,[22] but the thiol S-H band can be considered to be of use for general characterization. Therefore, most noteworthy is the appearance of band ÒIIÓ for R = 1, assigned to SH stretch vibrations (shown amplified in **Figure 6** insets). This reconfirms the presence of S bound in the form of thiol groups, as also identified via *N*-ethylmaleimide derivatization. The bands appearing in region ÒVÓ (around 1300 cm^{-1}) could also arise from sulfur-oxy compounds. Since the sulfur containing films were found to have very little (if any) oxygen this region can be rather attributed to CHx deformations as stated in **Table 1**.

Additionally, we note structural differences between the plasma- and VUV films, as also confirmed XPS data in the next sub-section.

High-resolution (HR-) XPS spectra

HR-XPS can help one to assess the nature of chemical bonding in the different films, before and after chemical derivatization. Possible bond types and their corresponding binding energies are shown in part a) of **Table 1**. **Figure 7**, typical C1s HR-XPS spectra for different films at R = 0.5 reveals two components: (i) aliphatic C-C and C-

H bonds (C1); and (ii) carbon-sulfur bonds (C2). For all films, the sub-peaks were placed at fixed binding energy positions relative to the C1 peak, following a procedure described by Girard-Lauriault et al..[23] To obtain the best overall fits, the Gaussian-Lorentzian product peak shape parameter was set at 30. Different types of S-bonding do not result in appreciable chemical shifts in the S2p HR-XPS spectrum, as the 2p electron of S in C-S, S-S and S-H bonds has a similar binding energy.[24]

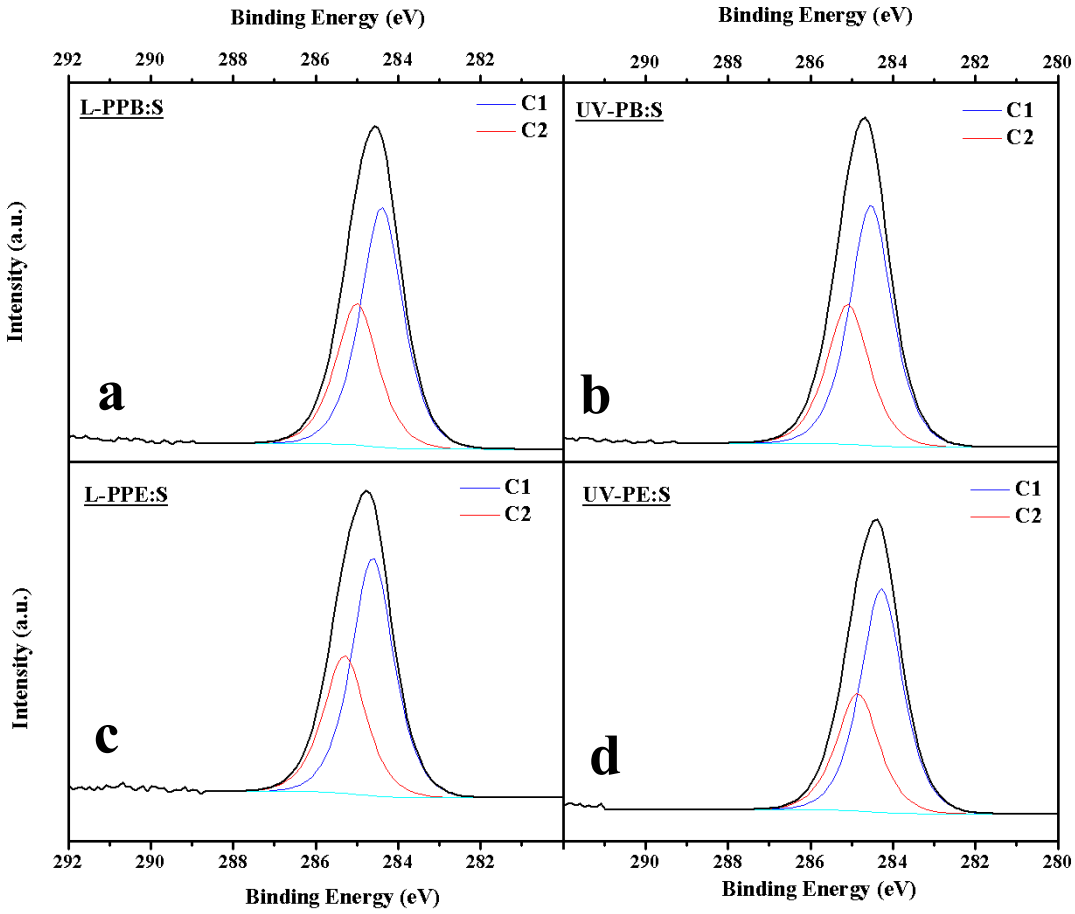

***Figure** 7 Typical high-resolution C1s XPS spectra of sulfur-containing deposits (R=0.5): a) L-PPB:S, b) UV-PB:S, c) L-PPE:S, d) UV-PE:S fitted with two component-peaks (FWHM 1.2 eV, peak shape GL(30)).*

In **Figure 8**, relative C1s peak fit component areas (in %) in four different films are shown plotted versus *R*.

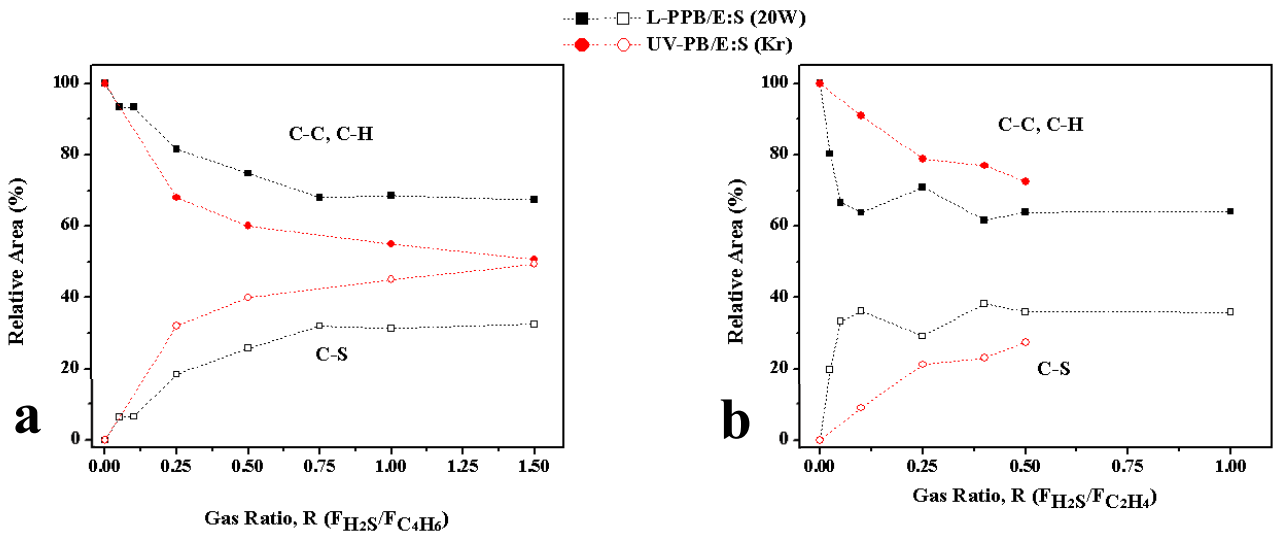

Figure 8 *Evolution of HR-XPS C1s peak fit components for a) L-PPB:S (squares, 20 W) and UV-PB:S (circles, KrL) and b) L-PPE:S (squares, 20 W) and UV-PE:S (circles, KrL) deposits as a function of gas mixture ratio, R. The lines are to guide the reader s eye.*

As before, the plasma- and VUV data for the C_4H_6- and C_2H_4-based films show similar behavior. **Figure 8a** is consistent with the XPS survey spectra, in that C-S peak intensity increases monotonically with rising *R*. **Figure 8b**, although less straightforward to interpret (especially for the plasma C_2H_4-based films), also shows an increase of the C-S peak intensity with rising *R*. The C1s peaks offer very few distinguishing features making it difficult to obtain information from these peaks. Therefore, the peak ~~deconvolution~~ fitting procedure is very sensitive to noise in the signal.

Assignments of likely chemical bonds after derivatization with *N*-ethylmaleimide are shown in part b) of **Table 1**, while typical high-resolution C 1s spectra are presented in **Figure 9**.

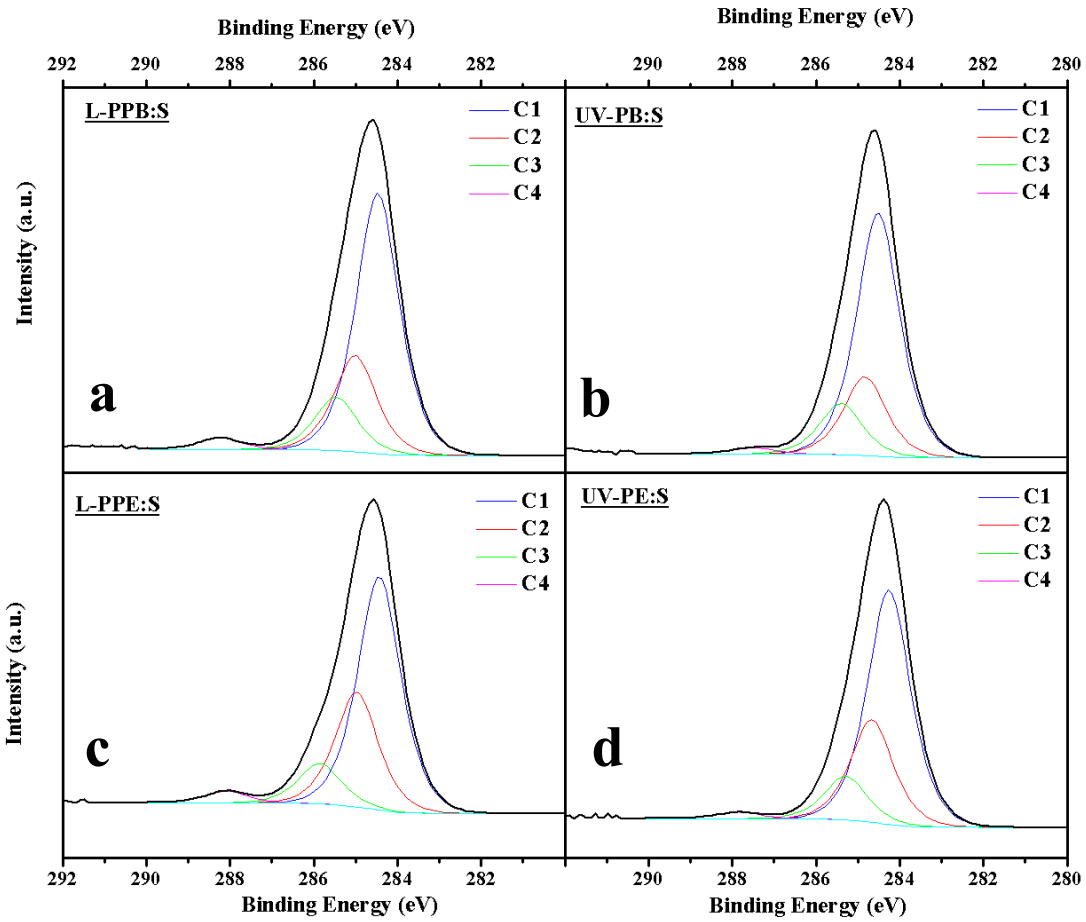

Figure 9 *High-resolution C1s XPS spectra of sulfur-containing deposits (R=0.5) after derivatization with N-ethylmaleimide: a) L-PPB:S, b) UV-PB:S, c) L-PPE:S, d) UV-PE:S fitted with four component-peaks (FWHM 1.2 eV, peak shape GL(30)).*

Unlike those in **Figure 7**, these now show additional components (C3 and C4, attributed to C-OR and ~~C-N=O~~ N-C=O) corresponding to new functionalities after derivatization (see **Scheme 1**).

Physico-chemical stability in water and toluene

The stability of plasma- and VUV-deposited coatings in aqueous media is of crucial importance if they are to be used in biomedical applications. Indeed, the stability of NH_2-containing coatings has been extensively discussed, and it was pointed out that

primary amines in those films oxidize to form other functional groups, such as amides, in the presence of water and atmospheric oxygen.[7b, 7c, 13] Moreover, high concentrations of bonded heteroatoms (N and/or O) increase the solubility of coatings in polar solvents (e.g. water). This is attributed to the presence of highly soluble, low molecular weight fractions formed during the deposition process, which are extractable in polar solvents.[25] In this context, it was also reported that VUV films tend to be less soluble than their plasma counterparts of comparable compositions, due to a higher cross-link density in the former that result from the photo-polymerization process.[7b]

All C_4H_6-based coatings (plasma- and VUV alike) ~~were found to be quite insoluble~~ showed limited solubility in Milli-Q water, for $0 \leq R \leq 1.5$, although data did show some scatter, and in one case (R = 0.5) a 20% loss in thickness (ΔT). A possible explanation of the high stability of these coatings might be a particularly high cross-link density resulting from the molecule's two double bonds. This seems to be supported by the slightly higher observed solubility of the C_2H_4-based (plasma- and VUV-) coatings, although the latter also manifested no clear solubility increase with rising R ($0 \leq R \leq 1.0$).

Immersion in toluene should in principle remove all ~~inorganic~~ elemental sulfur that might be present.[26] Considering that S bound in the form of thiol groups, [SH], accounts for at most 3% of [S] (see **Figure 4** and **5**), other S-based functionalities (or possibly even elemental sulfur) must certainly be present. Regrettably, these cannot be identified on the basis of (inexistent) chemical shifts in high-resolution XPS spectra (see **Figure 7**).

In **Figure 10**, changes in thickness, ΔT~~, and in [S]~~ are plotted versus R ($R \leq 0.6$) for both C_4H_6- ((**a**~~), (c)~~) and C_2H_4-based ((**b**~~), (d)~~) coatings.

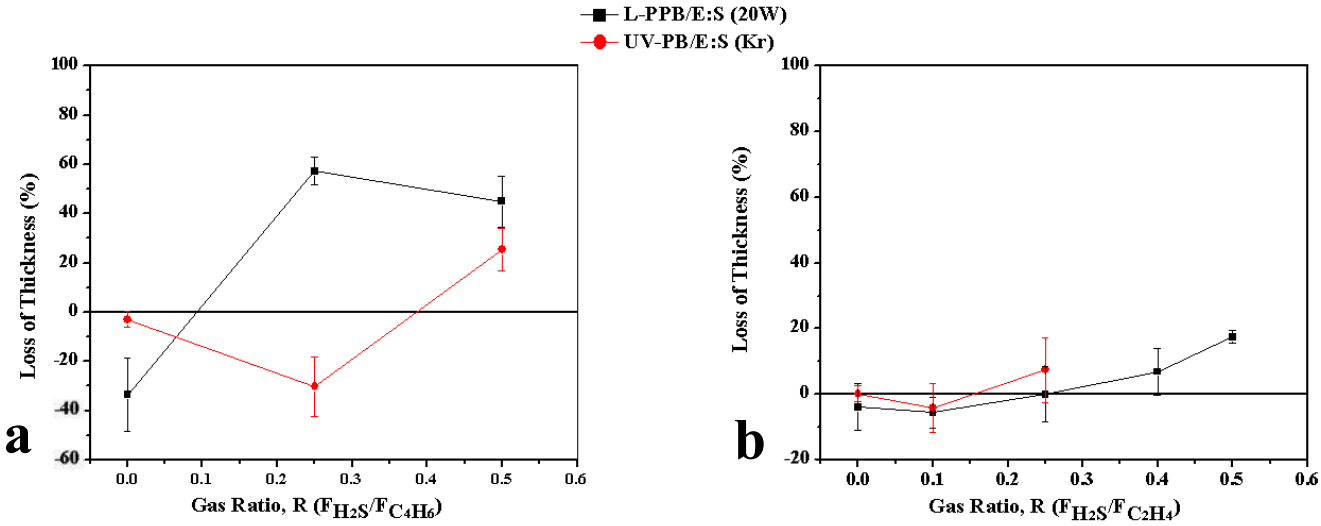

Figure 10 *Stability in toluene of as deposited L-PPB(E):S (squares, 20 W) and UV-PB(E):S (circles, KrL) films deposited using H_2S-C_4H_6(C_2H_4) mixtures. Loss of thickness, ΔT, (in %) of: a) L-PPB:S (squares, 20 W) and UV-PB:S (circles, KrL) and b) L-PPE:S (squares, 20 W) and UV-PE:S (circles, KrL) as a function of gas mixture ratio, R, after immersion in toluene for 24 h. Error bars show standard deviation of three measurements.*

Only relatively few data points have been taken, and Δ*T* manifests possible ambiguities (*negative* values, suggesting swelling, i.e. *gain* of *T*, as opposed to loss via dissolution). Comparing (**a**) and (**b**), the highest Δ*T* values, ca. 60% and 20%, are respectively noted for L-PPB:S ($R > 0.2$) and L-PPE:S ($R = 0.5$), while their VUV counterparts display significantly lower Δ*T* values, that is, greater stability in toluene. Indeed, the C_2H_4-based coatings appear to perform better.

In **Figure 11**, changes in [S] are plotted versus *R* ($R \leq 0.6$) for both C_4H_6- ((**a**)) and C_2H_4-based ((**b**)) coatings.

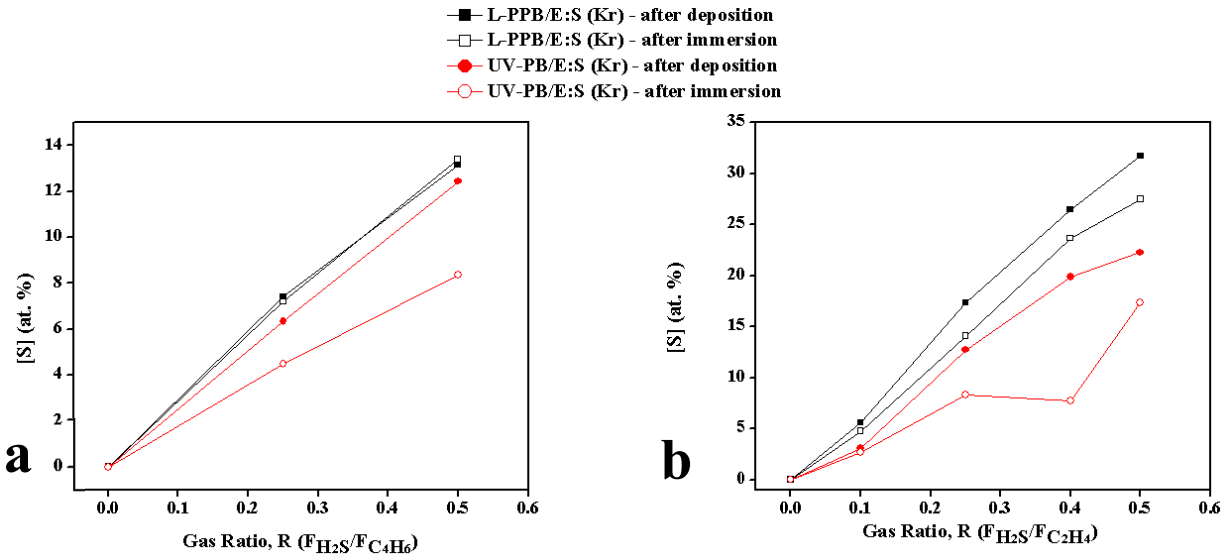

Figure 11 *Sulfur surface concentrations, [S] (XPS, in at. %), before (full symbols) and after (open symbols) immersion in toluene of ~~c~~a) L-PPB:S (squares, 20 W) and UV-PB:S (circles, KrL) and ~~d~~b) L-PPE:S (squares, 20 W) and UV-PE:S (circles, KrL) as a function of gas mixture ratio, R, after immersion in toluene for 24 h. The lines are to guide the reader s eye.*

~~Now turning to changes in [S] after immersion (compare (c) and (d)),~~ ~~t~~The following may be noted: Over the whole range of *R* values investigated, PP films systematically showed smaller reductions than their VUV counterparts. While there was virtually no change for L-PPB:S, UV-PB/E:S films displayed a change in [S] ~ - 10% at the higher *R* values. Compared with the ΔT data discussed above, this outcome is difficult to explain, particularly for the case of L-PPB:S (highest ΔT but lowest change in [S]).

General Discussion and Conclusions

While single-molecule precursors that incorporate the desired functionality have been used to create amine-, hydroxyl- and/or carboxyl-, and thiol-rich plasma-polymer

films, the 'co-polymerization' approach we present here for SH-containing films is unprecedented; it improves control over experimental outcome, and it can maximize the concentration of the desired functional group: We have demonstrated, to our knowledge for the first time, the possibility to create SH-terminated surfaces by co-polymerizing mixtures of a hydrocarbon (here C_4H_6 or C_2H_4) and H_2S by both vacuum-ultraviolet photo-initiated CVD and low-pressure r.f PECVD.

In **Figure 3** we noted that the deposition rates, *r*, of UV-PB/E:S and L-PPB/E:S coatings as a function of the gas mixture ratio, *R*, are quite different, the latter (plasma) method yielding higher *r* values. Such systematic differences were not apparent in regard to sulfur concentration, [S] (**Figure 4**), where we noted a monotonic increase with rising *R*, 2; [S]; 48 at. %. Furthermore, no significant distinction between photo- and plasma-polymerized films could be observed, beside that noted in **Figure 5**: the plasma-based coatings are seen to be richer in [SH] groups, up to ca. 3%. This result is somewhat surprising, considering that photo-polymerized coatings from C_2H_4-NH_3 mixtures presented in the literature proved to be highly amine (NH_2)-rich, with [NH_2]/[N] selectivity values exceeding 75%. Clearly, this does not apply in the case of C_2H_4 / H_2S or C_4H_6 / H_2S mixtures.

The different types of coatings were all found to be quite stable after 24 h of immersion in Milli-Q water, a key criterion for biomedical applications. Contrary to earlier reports for N- or O-rich coatings, we did not observe an increase in solubility with rising *R* values, nor significant differences between the photo- and plasma-polymerized coatings. Further stability tests conducted in toluene demonstrated that the sulfur in the films not in thiol form is likely of organic nature (**Figure 10**). ~~Unfortunately~~ Since the surfaces mainly showed non-oxidized sulfur, it is very

difficult to identify different types of S-bonding through HR-XPS, because chemical shifts in the S2p HR-XPS spectrum are not significant.

Butadiene-based coatings show great stability over a wide range of *R* values, confirming our hypothesis for using butadiene as a hydrocarbon source gas: its higher unsaturated structure compared with C_2H_4 presumably leads to more active species in 0the plasma, thereby increasing the cross-link density in the resulting coatings. ~~Indeed, C_2H_4-based coatings show lower stability, but they are more stable than previously reported amine-rich films.~~

In general, when comparing UV-PB/E:S and L-PPB/E:S coatings, all have proven to possess similar attributes, namely a high sulfur concentration, [S], and stability in water. The main differences occur in [-SH] values, the plasma-polymerized films being superior. Understanding this rather surprising result is of great interest, and it is the objective of ongoing further studies.

Acknowledgments: The authors gratefully acknowledge financial support from McGill University, from the *Fonds de recherche du Qu bec en nature et technologies* (FRQNT), and *Plasma-Qu bec*; from the Natural Sciences and Engineering Research Council of Canada (NSERC), and the Canadian Foundation for Innovation (CFI).

Received: ; Revised: ; Published online: DOI: 10.1002/ppap.201500200

Keywords: plasma polymerization; sulfur-rich organic films; thiol derivatization; vacuum ultraviolet photo-polymerization

[1] [a] Niklewski, A., Azzam, W., Strunskus, T., Fischer, R. A., Wšll, C., Langmuir 2004**,** 20, 20; [b] Guerin, D., Merckling, C., Lenfant, S., Wallart, X., Pleutin, S., Vuillaume, D., The Journal of Physical Chemistry C 2007**,** 111, 22; [c] Azzam, W., Wehner, B. I., Fischer, R. A., Terfort, A., Wšll, C., Langmuir 2002**,** 18, 21; [d] Smith, E. A., Wanat, M. J., Cheng, Y., Barreira, S. V. P., Frutos, A. G., Corn, R. M., Langmuir 2001**,** 17, 8.
[2] [a] Novotna, Z., Reznickova, A., Kvitek, O., Kasalkova, N. S., Kolska, Z., Svorcik, V., Applied Surface Science 2014**,** 307, 0; [b] Svorcik, V., Chaloupka, A., Zaruba, K., Kral, V., Blahova, O., Mackova, A., Hnatowicz, V., Nucl. Instrum. Methods Phys. Res. Sect. B-Beam Interact. Mater. Atoms 2009**,** 267, 15; [c] Kvitek, O., Bot, M., Svorcik, V., Applied Surface Science 2012**,** 258, 22; [d] Svorc'k, V., Kolska, Z., Siegel, J., Slepicka, P., Journal of Nano Research 2013**,** 25.
[3] [a] Schofield, W. C. E., McGettrick, J., Bradley, T. J., Badyal, J. P. S., Przyborski, S., J. Am. Chem. Soc. 2006**,** 128, 7; [b] Harris, L. G., Schofield, W. C. E., Badyal, J. P. S., Chem. Mat. 2007**,** 19, 7; [c] Muguruma, H., Plasma Process. Polym. 2010**,** 7, 2.
[4] Harris, L. G., Schofield, W. C. E., Doores, K. J., Davis, B. G., Badyal, J. P. S., J. Am. Chem. Soc. 2009**,** 131, 22.
[5] Weinrich, D., Lin, P. C., Jonkheijm, P., Nguyen, U. T., Schroder, H., Niemeyer, C. M., Alexandrov, K., Goody, R., Waldmann, H., Angew Chem Int Ed Engl 2010**,** 49, 7.
[6] [a] Jonkheijm, P., Weinrich, D., Kšhn, M., Engelkamp, H., Christianen, P. C. M., Kuhlmann, J., Maan, J. C., NŸsse, D., Schroeder, H., Wacker, R., Breinbauer, R., Niemeyer, C. M., Waldmann, H., Angewandte Chemie 2008**,** 120, 23; [b] Lin, P. C., Ueng, S. H., Tseng, M. C., Ko, J. L., Huang, K. T., Yu, S. C., Adak, A. K., Chen, Y. J., Lin, C. C., Angew. Chem.-Int. Edit. 2006**,** 45, 26.
[7] [a] Wertheimer, M. R., St-Georges-Robillard, A., Lerouge, S., Mwale, F., Elkin, B., Oehr, C., Wirges, W., Gerhard, R., Jpn. J. Appl. Phys. 2012**,** 51, 11; [b] Ruiz, J.-C., St-Georges-Robillard, A., ThŽrŽsy, C., Lerouge, S., Wertheimer, M. R., Plasma Process. Polym. 2010**,** 7, 9-10; [c] Truica-Marasescu, F., Ruiz, J.-C., Wertheimer, M. R., Plasma Process. Polym. 2012**,** 9, 5; [d] Truica-Marasescu, F., Wertheimer, M. R., Macromolecular Chemistry and Physics 2008**,** 209, 10.
[8] [a] Thiry, D., Francq, R., Cossement, D., Guerin, D., Vuillaume, D., Snyders, R., Langmuir 2013**,** 29, 43; [b] Thiry, D., Britun, N., Konstantinidis, S., Dauchot, J. P., Denis, L., Snyders, R., Appl. Phys. Lett. 2012**,** 100, 7; [c] Thiry, D., Francq, R., Cossement, D., Guillaume, M., Cornil, J., Snyders, R., Plasma Process. Polym. 2014**,** 11, 6.
[9] [a] Hollander, A., Kropke, S., Plasma Process. Polym. 2010**,** 7, 5; [b] Siow, K. S., Kumar, S., Griesser, H. J., Plasma Process. Polym. 2015**,** 12, 1; [c] Gugala, Z., Gogolewski, S., J. Biomed. Mater. Res. Part A 2006**,** 76A, 2.
[10] [a] Truica-Marasescu, F., Pham, S., Wertheimer, M. R., Nuclear Instruments and Methods in Physics Research Section B: Beam Interactions with Materials and Atoms 2007**,** 265, 1; [b] Ruiz, J.-C., Girard-Lauriault, P.-L., Truica-Marasescu, F., Wertheimer, M. R., Radiation Physics and Chemistry 2010**,** 79, 3; [c] Contreras-Garcia, A., Wertheimer, M. R., Plasma Chem. Plasma Process. 2013**,** 33, 1.
[11] Yasuda, H., *Plasma polymerization*. Academic Press: Orlando, 1985.

[12] [a] Hossain, M. M., MŸssig, J., Herrmann, A. S., Hegemann, D., J. Appl. Polym. Sci. 2009**,** 111, 5; [b] Hegemann, D., Kšrner, E., Albrecht, K., SchŸtz, U., Guimond, S., Plasma Process. Polym. 2010**,** 7, 11; [c] Hegemann, D., Hossain, M.-M., Plasma Process. Polym. 2005**,** 2, 7; [d] Korner, E., Fortunato, G., Hegemann, D., Plasma Process. Polym. 2009**,** 6, 2.
[13] Ruiz, J. C., Girard-Lauriault, P. L., Wertheimer, M. R., Plasma Process. Polym. 2015**,** 12, 3.
[14] Okabe, H., *Photochemistry of Small Molecules*. John Wiley & Sons: New York, 1978.
[15] [a] Fahr, A., Laufer, A. H., Journal of Photochemistry 1986**,** 34, 3; [b] Holland, D. M. P., Shaw, D. A., Hayes, M. A., Shpinkova, L. G., Rennie, E. E., Karlsson, L., Baltzer, P., Wannberg, B., Chemical Physics 1997**,** 219, 1.
[16] [a] Fahr, A., Nayak, A. K., Chemical Physics 1994**,** 189, 3; [b] Schoen, R. I., The Journal of Chemical Physics 1962**,** 37, 9.
[17] Robinson, J. C., Harris, S. A., Sun, W. Z., Sveum, N. E., Neumark, D. M., J. Am. Chem. Soc. 2002**,** 124, 34.
[18] [a] Truica-Marasescu, F., Wertheimer, M. R., J. Appl. Polym. Sci. 2004**,** 91, 6; [b] Truica-Marasescu, F.-E., Wertheimer, M. R., Macromolecular Chemistry and Physics 2005**,** 206, 7; [c] Truica-Marasescu, F., Guimond, S., Jedrzejowski, P., Wertheimer, M. R., Nuclear Instruments and Methods in Physics Research Section B: Beam Interactions with Materials and Atoms 2005**,** 236, 1-4.
[19] Yong, Chun Q., Jongryang Joo, Donggeun Jung, Jpn. J. Appl. Phys. 1999**,** 38, 3R.
[20] Beamson, G., Briggs, D., *High resolution XPS of organic polymers : the Scienta ESCA300 database*. Wiley: Chichester [England]; New York, 1992.
[21] Lin-Vien, D., Colthup, N. B., Fateley, W. G., Grasselli, J. G., 1991.
[22] Coates, J., Encyclopedia of analytical chemistry 2000.
[23] Girard-Lauriault, P. L., Dietrich, P. M., Gross, T., Wirth, T., Unger, W. E. S., Plasma Process. Polym. 2013**,** 10, 4.
[24] [a] Gardella, J. A., Ferguson, S. A., Chin, R. L., Appl. Spectrosc. 1986**,** 40, 2; [b] Peisert, H., ChassŽ, T., Streubel, P., Meisel, A., Szargan, R., Journal of Electron Spectroscopy and Related Phenomena 1994**,** 68; [c] Volmer, M., Stratmann, M., Viefhaus, H., Surface and Interface Analysis 1990**,** 16, 1-12.
[25] [a] Zhang, Z., Chen, Q., Knoll, W., Forch, R., Surf. Coat. Technol. 2003**,** 174; [b] Vasilev, K., Britcher, L., Casanal, A., Griesser, H. J., J. Phys. Chem. B 2008**,** 112, 35.
[26] [a] Ren, Y. Q., Shui, H. Z., Peng, C. J., Liu, H. L., Hu, Y., Fluid Phase Equilib. 2011**,** 312; [b] Jay, S., Cezac, P., Serin, J. P., Contamine, F., Martin, C., Mercadier, J., J. Chem. Eng. Data 2009**,** 54, 12; [c] Steudel, R.; SpringerLink, 2003.

Sulfur-rich organic thin films were synthesized by co-polymerizing gas mixtures of H_2S and C_4H_6, as well as H_2S and C_2H_4, using low-pressure r.f. plasma-enhanced CVD and vacuum ultraviolet (VUV) photo-polymerization. Analyses of the different films were performed by XPS and by IRRAS-FTIR. VUV- and plasma coatings possess similar structures and characteristics yielding sulfur concentrations up to 48 at.%.

Evelyne Kasparek, Jason R. Tavares, Michael R. Wertheimer, Pierre-Luc Girard-Lauriault*

Sulfur-rich Organic Films deposited by Plasma- and Vacuum-ultraviolet (VUV) Photo-polymerization